ORIGINAL ARTICLE

Leucine treatment enhances oxidative capacity through complete carbohydrate oxidation and increased mitochondrial density in skeletal muscle cells

Roger A. Vaughan · Randi Garcia-Smith ·
Nicholas P. Gannon · Marco Bisoffi ·
Kristina A. Trujillo · Carole A. Conn

Abstract Leucine has been largely implicated for increasing muscle protein synthesis in addition to stimulating mitochondrial biosynthesis. Limited evidence is currently available on the effects and potential benefits of leucine treatment on skeletal muscle cell glycolytic and oxidative metabolism. This work identified the effects of leucine treatment on oxidative and glycolytic metabolism as well as metabolic rate of human and murine skeletal muscle cells. Human rhabdomyosarcoma cells (RD) and mouse myoblast cells (C2C12) were treated with leucine at either 100 or 500 μM for 24 or 48 h. Glycolytic metabolism was quantified by measuring extracellular acidification rate (ECAR) and oxidative metabolism was quantified by measuring oxygen consumption rate. Peroxisome proliferator-activated receptor coactivator 1 alpha (PGC-1α), an important stimulator of mitochondrial biosynthesis, was quantified using flow cytometry and verified by immunofluorescent confocal microscopy. Mitochondrial content was quantified using mitochondrial and cytochrome C staining measured by flow cytometry and confirmed with confocal microscopy. Treatment with leucine significantly increased both basal and peak oxidative metabolism in both cell models. Leucine treated cells also exhibited significantly greater mitochondrial proton leak, which is associated with heightened energy expenditure. Basal ECAR was significantly reduced in both cell models following leucine treatment, evidence of reduced lactate export and more complete carbohydrate oxidation. In addition, both PGC-1α and cytochrome C expression were significantly elevated in addition to mitochondrial content following 48 h of leucine treatment. Our observations demonstrated few dose-dependent responses induced by leucine; however, leucine treatment did induce a significant dose-dependent expression of PGC-1α in both cell models. Interestingly, C2C12 cells treated with leucine exhibited dose-dependently reduced ATP content, while RD ATP content remain unchanged. Leucine presents a potent dietary constituent with low lethality with numerous beneficial effects for increasing oxidative preference and capacity in skeletal muscle. Our observations demonstrate that leucine can enhance oxidative capacity and carbohydrate oxidation efficiency, as well as verify previous observations of increased mitochondrial content.

Keywords Mitochondrial biosynthesis · PGC ·
Extracellular acidification and oxygen consumption rates ·
Oxidative phosphorylation · Dietary supplements

R. A. Vaughan (✉)
Department of Health, Exercise and Sports Science,
University of New Mexico, 1 University Blvd, Albuquerque,
NM 87131, USA
e-mail: vaughanr@unm.edu

R. A. Vaughan · R. Garcia-Smith · N. P. Gannon · M. Bisoffi ·
K. A. Trujillo
Department of Biochemistry and Molecular Biology,
University of New Mexico Health Sciences Center,
Albuquerque, NM 87131, USA
e-mail: randigarcia@salud.unm.edu

N. P. Gannon
e-mail: ngannon@unm.edu

M. Bisoffi
e-mail: mbisoffi@salud.unm.edu

K. A. Trujillo
e-mail: ktrujillo@salud.unm.edu

R. A. Vaughan · C. A. Conn
Department of IFCE: Nutrition, University of New Mexico,
Albuquerque, NM 87131, USA
e-mail: cconn@unm.edu

Background

Leucine is a branched-chain amino acid that is essential in the human diet. Leucine has become a popular dietary supplement and constituent of many performance-enhancing sports powders and products. Leucine is heavily researched for its ability to promote protein synthesis resulting in increased skeletal muscle anabolism. Previous work has documented the effects of leucine on peroxisome proliferator-activated receptor coactivator 1 alpha (PGC-1α) expression, mitochondrial biosynthesis, and increased metabolic rate (Sun and Zemel 2007, 2009; Zhang et al. 2007). The mechanism by which leucine acts to increase mitochondrial content via PGC activation is not currently understood, although there have been observations that leucine activates silent information regulator transcript 1 (SIRT1). In addition, there is a common hypothesis that leucine treatment of cells in vitro results in greater mitochondrial content to support the heightened energy needs of increased protein synthesis which is uniquely stimulated by leucine (Sun and Zemel 2007, 2009). It has been previously observed that leucine treatment of cultured C2C12 mouse myoblasts results in heightened oxygen consumption, an indirect measure of oxidative metabolism (Sun and Zemel 2007, 2009). There is, however, no evidence evaluating the effect of leucine on other metabolic dynamics including glycolytic capacity. Our lab has previously investigated the metabolic consequences of numerous dietary and pharmacological chemicals on skeletal muscle metabolism and mitochondrial content (Vaughan et al. 2012a, b, c). This work specifically investigated the effects of leucine treatment on peak mitochondrial metabolism, as well as basal and peak glycolytic capacity. In addition, we measured changes in mitochondrial content, ATP production, and metabolic gene expression.

Methods

Cell culture

Homo sapiens rhabdomyosarcoma (RD) cells and mouse myoblast (C2C12) cells were purchased from ATCC (Manassas, VA). RD and C2C12 cells are naturally immortalized cell models, frequently used for making inferences about muscle tissue adaptations (Araki et al. 2012; Armoni et al. 2002; Lendoye et al. 2011; Pagel-Langenickel et al. 2008; Philp et al. 2011; Singh et al. 2010; Vaughan et al. 2012b). Cells were cultured in Dulbecco's Modified Eagle's Medium (DMEM) containing 4,500 mg/L glucose and supplemented with 10 % heat-inactivated fetal bovine serum (FBS) and 100 U/mL

penicillin/streptomycin, in a humidified 5 % CO_2 atmosphere at 37 °C. Stock leucine from Sigma (St. Louis, MO) was dissolved in culture media and diluted to either 100 or 500 μM (as determined through pilot data and previous observations) (Sun and Zemel 2009). Dose was determined through pilot experiments and previous observations which correspond to physiological levels following leucine consumption, and exposure times were determined through pilot experiments and through previously reported observations (Sun and Zemel 2009). Similar observations in C2C12 myoblasts and cultured adipocytes have discerned that metabolic effects of leucine are a result of unique characteristics that are not found in similar amino acids such as valine (Sun and Zemel 2009). To verify these observations, we conducted all metabolic observations with valine, an isonitrogenous branched-chain amino acid at 500 μM for 24 h which revealed no change in any metabolic parameters measured (data not shown).

Flow cytometry

Cells were plated in 6-well plates at a density of 1.0×10^6 cells/well treated in triplicate and incubated as previously described above for 48 h. Following treatment, the media was removed and the cells were resuspended in pre-warmed media with 200-nM Mitotracker Green from Life Technologies (Carlsbad, CA) and incubated for 45 min in a humidified 5 % CO_2 atmosphere at 37 °C. The cells were pelleted, the media with Mitotracker was removed and the cells were suspended in pre-warmed media. Group mean fluorescence was measured using Facscalibur filtering 488 nm. To quantify PGC-1α and cytochrome C expression, we used immunofluorescent staining measured by flow cytometry. Cells were permeabilized with PBS with 0.1 % Tween from Sigma (St. Louis, MO) for 10 min and blocked for 1 h with PBS with 0.1 % Tween and 3.0 % BSA from Sigma (St. Louis, MO). Cells were stained with either an anti-PGC-1α polyclonal or anti-CytC monoclonal primary antibody from Santa Cruz Biotechnologies (Santa Cruz, CA) at 1:200 dilution in PBS with 0.1 % BSA overnight. The cells were rinsed with PBS with 0.1 % Triton 100X and 3.0 % BSA, and secondary anti-rabbit AlexaFluor 488 or a secondary anti-mouse AlexaFluor 488 antibody from Invitrogen (Carlsbad, CA) was applied in 1:200 dilutions. Cells were rinsed thoroughly and fluorescence was measured via flow cytometry.

Microscopy and immunohistochemistry

Chamber-slides from BD Bioscience (Sparks, MD), were seeded with 5,000 cells/well. To verify PGC-1α protein expression, cells were cultured and treated for 48 h as

described above. Cells were fixed using 3.7 % formal-dehyde in media, permeabilized with PBS with 0.1 % Triton 100X from Sigma (St. Louis, MO) for 10 min and blocked for 1 h with PBS with 0.1 % Triton 100X and 3.0 % BSA from Sigma (St. Louis, MO). Cells were stained with either an anti-PGC-1α or anti-CytC primary antibody from Santa Cruz Biotechnologies (Santa Cruz, CA) at 1:200 dilution in PBS with 0.1 % BSA overnight. The cells were rinsed with PBS with 0.1 % Triton 100X and 3.0 % BSA, and a secondary anti-rabbit AlexaFluor 633 or a secondary anti-mouse antibody from Invitrogen (Carlsbad, CA) was applied in 1:200 dilution. Slides were mounted with Prolong Gold with DAPI from Invitrogen (Carlsbad, CA) and cured overnight. Cells were imaged using the Axiovert 25 microscope with AxioCam MRc from Zeiss (Thornwood, NY). To verify increased mitochondrial content, the cells were stained with Mitotracker 200 nM from Invitrogen (Carlsbad, CA) for 45 min, and fixed in 3.7 % formaldehyde in pre-warmed media. Cells were mounted, cured, and imaged as described above.

Metabolic assay

Cells were seeded overnight in 24-well culture plate from SeaHorse Bioscience (Billerica, MA) at density 5×10^5 cells/well (RD cells) or 2.5×10^5 (C2C12 cells), treated and incubated for 24 h as described above. Following treatment, culture media was removed and replaced with XF Assay Media from SeaHorse Bioscience (Billerica, MA) containing 4,500 mg/L glucose free of CO_2 and incubated at 37 °C. Per manufactures' protocol, SeaHorse injection ports were loaded with oligomycin, an inhibitor of ATP synthase which induces maximal glycolytic metabolism and reveals endogenous proton leak (mitochondrial uncoupling) at a final concentration 1.0 μM. Oligomycin addition was followed by the addition of carbonyl cyanide p-[trifluoromethoxy]-phenyl-hydrazone (FCCP), an uncoupler of electron transport that induces peak oxygen consumption (an indirect indicator of peak oxidative metabolism) at final concentration 1.25 μM. Rotenone was then added in 1.0-μM final concentration to reveal non-mitochondrial respiration and end the metabolic reactions (Giulivi et al. 2008; Wikstrom et al. 2012). Extracellular acidification, an indirect measure of glycolytic capacity, and oxygen consumption, a measure of oxidative metabolism was measured using the SeaHorse XF24 Extracellular Analyzer from SeaHorse Bioscience (Billerica, MA). Sea-Horse XF24 Extracellular Analyzer was run using 8-min cyclic protocol commands (mix for 3 min, let stand 2 min, and measure for 3 min) in triplicate.

Cellular ATP content

Cells were seeded overnight in a 6-well plate at density 1×10^6 cells/well and treated as described above for 48 h. The cells were lysed in 1 % CHAPS lysis buffer from Chemicon (Billerica, MA) in PBS with Ca^{2+} and MG^{2+} and the ATP-containing supernatant was recovered. Samples were allocated into a 96-well plate with a 1:1 dilution of ATP Bioluminescence Reagent from Sigma (St. Louis, MO) with a 100-μM final volume and luminescence was measured and normalized to serial dilutions of ATP. ATP concentrations were normalized to cell density determined through hemocytometer measured by staining cells with trypan blue from Sigma (St Louis, MO) with cell density estimated using a Countess™ cell quantification system from Invitrogen (Carlsbad, CA).

Cell viability

Cells were seeded in 96-well plates at density 5,000 cells/well and grown overnight. Cells were treated and incubated as previously described for 48 h. Media and treatment were removed and media containing 10 % WST1 was added to each well and were incubated as previously described. Fluorescence was measured 1 h following WST1 addition using Wallac Victor3V 1420 Multilabel Counter from PerkinElmer (Waltham, MA).

Statistical analysis

Flow cytometry, metabolic assays, and cell viability were analyzed using ANOVA with Dunnett's post-hoc test and pairwise comparisons were used to compare treatments with control. Values of $p < 0.05$ indicated statistical significance in all tests and Prism from GraphPad (La Jolla, CA) was used to perform all statistical analyses.

Results

Metabolic adaptations

In order to assess changes in oxidative metabolism we measured oxygen consumption rate (OCR), an indirect indicator of mitochondrial metabolism. Treatment of C2C12 cells with leucine at either 100 or 500 μM for 24 h increased both basal and peak oxidative metabolism (Fig. 1a, b, respectively). Similarly, RD cells exhibited an increase in both basal and peak oxidative metabolism (Fig. 1c, d, respectively). Interestingly, C2C12 cells treated with leucine exhibited significantly increased mitochondrial uncoupling (Fig. 2a) which was not observed in treated RD cells (Fig. 2c). Non-mitochondrial oxygen consumption was

significantly elevated in both RD and C2C12 cells following 24-h leucine treatment, and there was a significant dose-dependent response in the RD cell model (Fig. 2b, d).

In order to assess changes in glycolytic metabolism, we measured extracellular acidification rate (ECAR). Both RD and C2C12 cells exhibited significantly reduced basal glycolytic metabolism following treatment with leucine for 24 h, and a significant dose-dependent relationship was identified in the C2C12 cell model (Fig. 3a, c). Peak glycolytic metabolism was also reduced in both cell models (Fig. 3b, d). Oxidative metabolic reliance expressed as a ratio of OCR:ECAR was also significantly altered following leucine treatment for 24 h. Specifically, C2C12 cells had a significantly elevated basal and peak oxidative reliance induced by both concentrations of leucine (Fig. 4a, b, respectively). Both basal and peak oxidative metabolic reliance was increased by leucine treatment at 100 μM, but not at 500 μM (Fig. 4c, d, respectively).

Cellular ATP content

In order to further evaluate the effects of leucine treatment on cellular metabolism, we measured cellular ATP content. C2C12 myocytes treated with leucine exhibited significantly reduced cellular ATP content compared with the control (Fig. 5a). RD cells treated with leucine did not display altered ATP content (Fig. 5b).

Mitochondrial adaptations

In order to evaluate the effect of altered metabolism on mitochondrial content, we measured PGC-1α and cytochrome C expression via immunofluorescence by flow cytometry and confocal microscopy. RD cells treated with leucine exhibited significantly greater dose-dependent increase in PGC-1α expression (Fig. 6a) which was verified by confocal microscopy (Fig. 6b). Similarly C2C12 cells treated with leucine had significantly greater PGC-1α expression compared with control cells (Fig. 6c) which was verified by confocal microscopy (Fig. 6d). In addition, we measured the effects of leucine treatment on cytochrome C expression. Leucine treatment of RD cells resulted in significantly greater dose-dependent increase cytochrome C expression compared with control (Fig. 7a) verified by microscopy (Fig. 7b). C2C12 cells treated with leucine displayed significantly greater dose-dependent increase cytochrome C staining compared with the control (Fig. 7c, d). To confirm our observations of increased mitochondrial density following leucine treatment, we stained cells with Mitotracker Green. RD cells treated with leucine had significantly greater

Fig. 1 Oxidative metabolism. a Basal oxidative metabolism expressed as oxygen consumption rate (OCR) of C2C12 cells treated with either 100 or 500 μM for 24 h. 95 % CI = control vs. leucine 100 μM: −149.8 to −92.22 and control vs. leucine 500 μM: −90.78 to –33.22. b Peak oxidative metabolism of C2C12 cells treated as described above for 24 h. 95 % CI = control vs. leucine 100 μM: −287.2 to −176.8 and control vs. leucine 500 μM: −289.2 to −178.8. c Basal oxidative metabolism of RD cells treated with either 100 or 500 μM for 24 h. 95 % CI = control vs. leucine 100 μM: −188.2 to −7.813 and control vs. leucine 500 μM: −121.2 to 59.19. d Peak oxidative metabolism of RD cells treated as described above. 95 % CI = control vs. leucine 100 μM: −255.7 to −100.3 and control vs. leucine 500 μM: −269.7 to −114.3. *$p < 0.05$, **$p < 0.01$, and ***$p < 0.001$ significantly greater than control
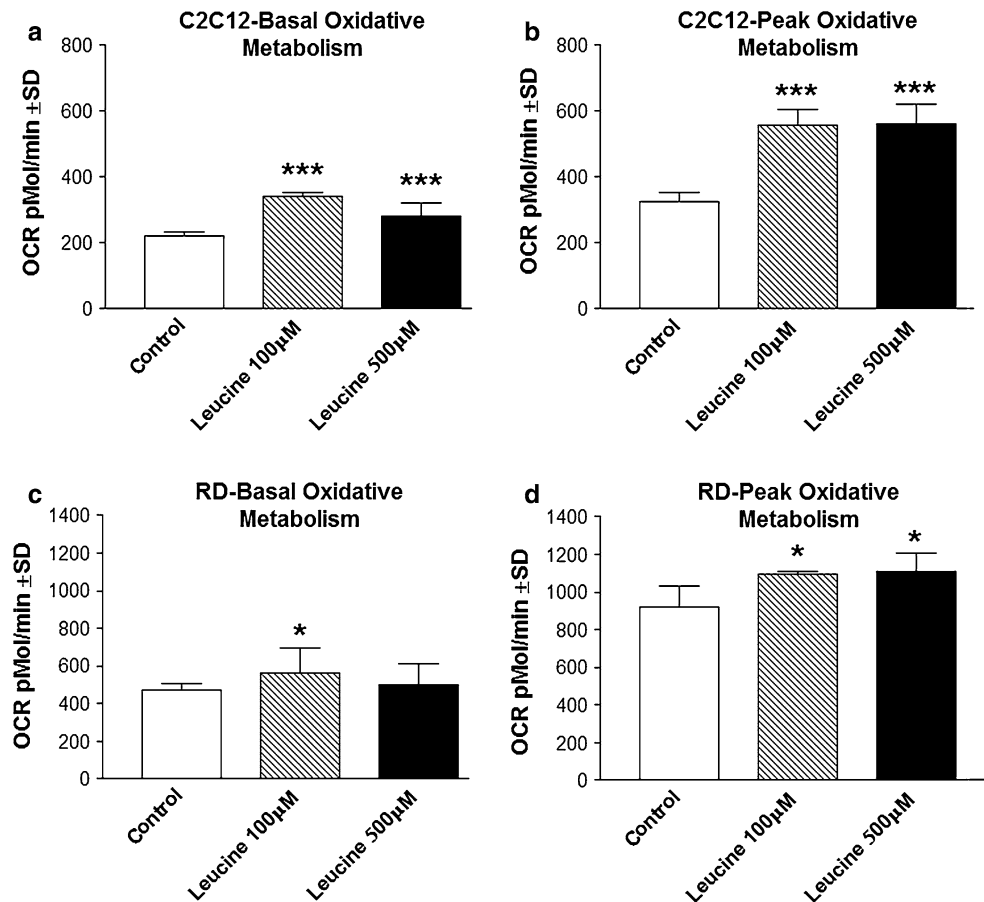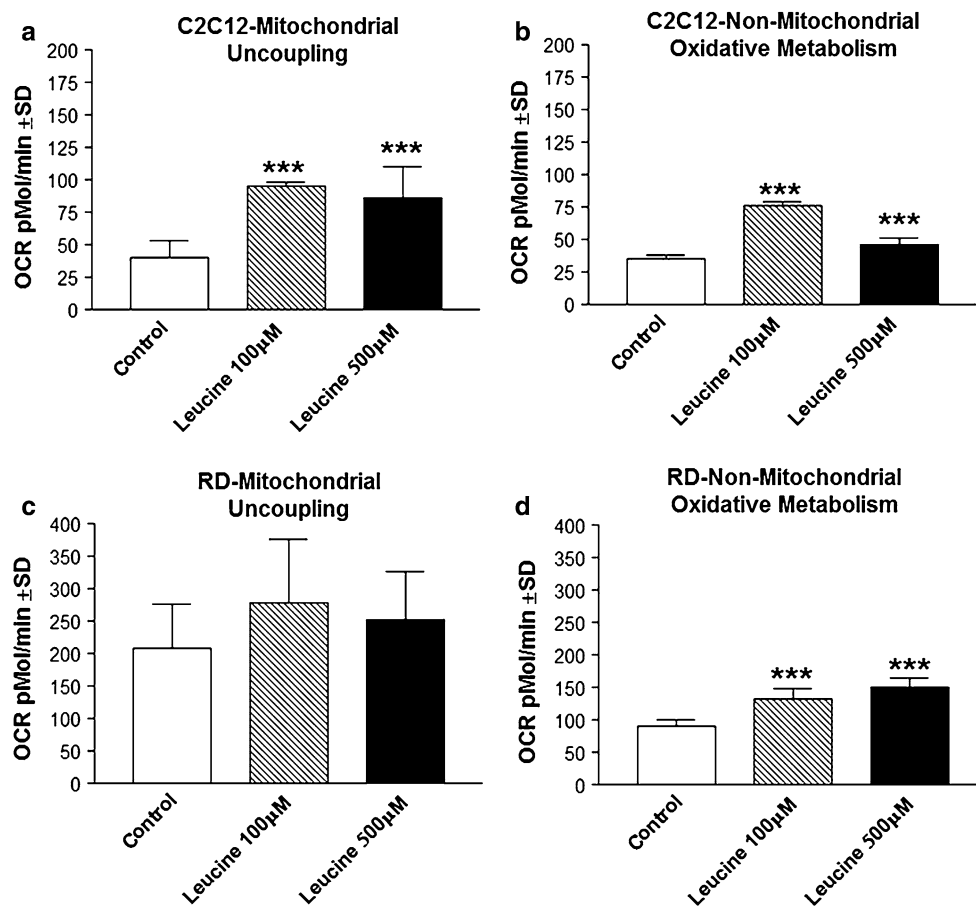
Fig. 2 Mitochondrial uncoupling and non-mitochondrial metabolism. **a** Mitochondrial proton leak (uncoupling) expressed as oxygen consumption rate (OCR) of C2C12 cells treated with either 100 or 500 μM for 24 h following addition of oligomycin. 95 % CI = control vs. leucine 100 μM: −73.08 to −36.92 and control vs. leucine 500 μM: −64.08 to −27.92. **b** Non-mitochondrial oxygen consumption of C2C12 cells treated as described above for 24 h following addition of rotenone. 95 % CI = control vs. leucine 100 μM: −45.06 to −36.94 and control vs. leucine 500 μM: −15.06 to −6.938. **c** Mitochondrial proton leak (uncoupling) expressed as oxygen consumption rate (OCR) of RD cells treated with either 100 or 500 μM for 24 h following addition of oligomycin. 95 % CI = control vs. leucine 100 μM: −141.3 to 1.278 and control vs. leucine 500 μM: −115.3 to 27.28. **d** Non-mitochondrial oxygen consumption of C2C12 cells treated as described above for 24 h following addition of rotenone. 95 % CI = control vs. leucine 100 μM: −53.69 to −30.31 and control vs. leucine 500 μM: −71.69 to −48.31. $^*p < 0.05$, $^{**}p < 0.01$, and $^{***}p < 0.001$ significantly greater than control

mitochondrial staining than control observed in both flow cytometry and microscopy (Fig. 8a, b). These findings were also seen for C2C12 cells treated with leucine (Fig. 8c, d).

Cell viability

In order to assess changes in cell viability, we used WST1 metabolic assay, an indirect indicator of cell proliferation and viability. RD and C2C12 cell viability was not significantly different between control and cell treated with leucine for 48 h (Fig. 9a, b).

Discussion

Leucine is a primary component in many dietary supplements, and is a viable therapeutic possibility because of its essential nature and limited toxicity. At the present time, benefits for humans consuming excess leucine beyond the essential amino acids found in protein are still unclear, although substantial in vitro work supports the hypothesis of possible metabolic benefits (Atherton et al. 2010; Deldicque et al. 2008; Du et al. 2007; Glynn et al. 2010; Haegens et al. 2012; Sun and Zemel 2007, 2009; Zhang et al. 2007). Leucine is currently of great interest because of its profound influence on protein synthesis in skeletal muscle through stimulation of mammalian target of rapamycin (mTOR) and impedance of Akt phosphorylation (Atherton et al. 2010; Deldicque et al. 2008; Du et al. 2007; Glynn et al. 2010; Haegens et al. 2012). Our observations pursued the less-studied effects of leucine on metabolic tendencies in muscle cells. We confirmed previous findings that leucine treatment increases basal cellular oxidative metabolism

Fig. 3 Glycolytic metabolism. **a** Basal glycolytic metabolism expressed as extracellular acidification rate (ECAR) of C2C12 cells treated with either 100 or 500 μM for 24 h. 95 % CI = control vs. leucine 100 μM: 0.5515–3.449 and control vs. leucine 500 μM: 4.551–7.449. **b** Peak glycolytic metabolism of C2C12 cells treated as described above for 24 h. 95 % CI = control vs. leucine 100 μM: 0.3862–5.614 and control vs. leucine 500 μM: 0.3862–5.614. **c** Basal glycolytic metabolism of RD cells treated with either 100 or 500 μM for 24 h. 95 % CI = control vs. leucine 100 μM: 8.222–33.78 and control vs. leucine 500 μM: 5.222–30.78. **d** Peak glycolytic metabolism of RD cells treated as described above. 95 % CI = control vs. leucine 100 μM: 9.040–16.96 and control vs. leucine 500 μM: 4.040–11.96. $^{†}p < 0.05$, $^{††}p < 0.01$, and $^{†††}p < 0.001$ significantly less than control
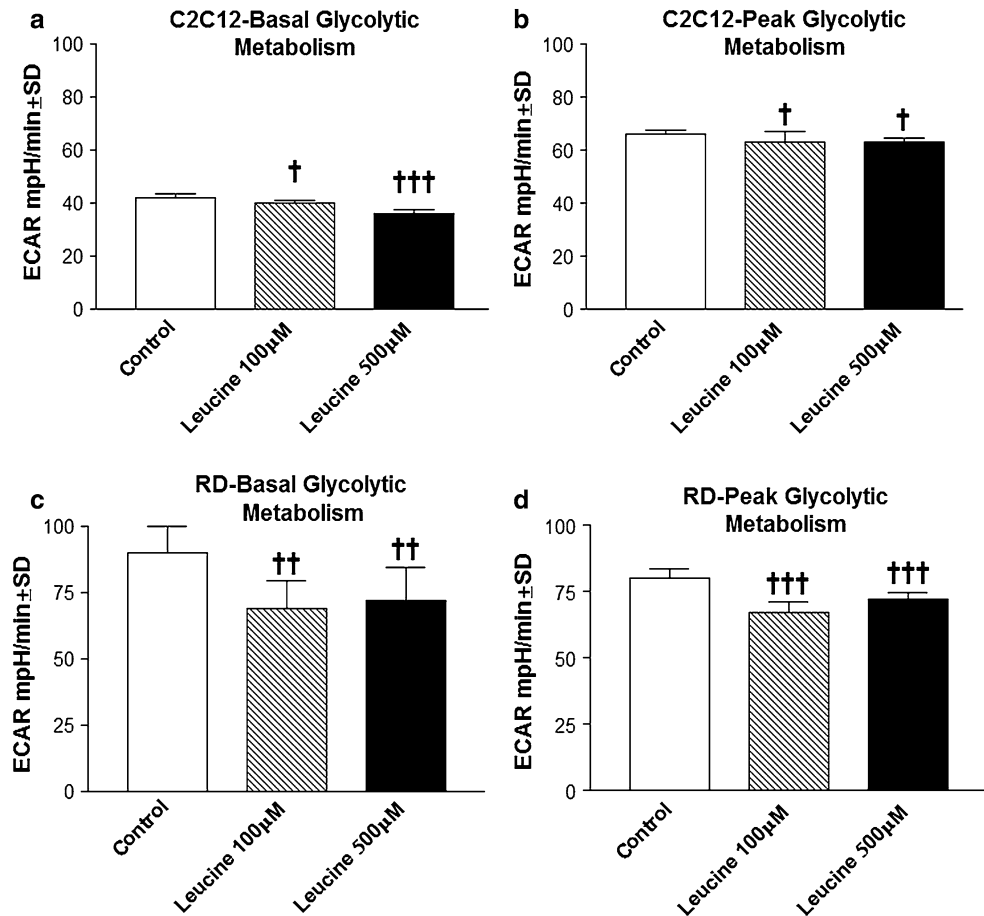
and mitochondrial content of various cultured muscle cells (Sun and Zemel 2007, 2009). Uniquely, our observations demonstrate that leucine can enhance peak oxidative metabolism chemically induced by FCCP, as well as endogenous mitochondrial uncoupling and oxidative reliance in cultured skeletal muscle cells, a powerful determinant of metabolic rate. This supports the previous observation that leucine can enhance endogenous mitochondrial uncoupling protein expression in skeletal muscle cells (Sun and Zemel 2009). Moreover, we demonstrated that leucine treatment increases complete carbohydrate metabolism through oxidation during both basal and peak glycolytic conditions, evidenced by reduction in extracellular acidification and heightened oxygen consumption in cells cultured in high-glucose conditions (see Figs. 3, 4). It is, however, meaningful that much of our experiments did not yield significant dose-dependence of leucine dose, suggesting that the effects of leucine are saturable. Despite this saturating effect, we hypothesize that leucine functions through multiple pathways to heighten energy expenditure simultaneously. Specifically, we hypothesize that leucine promotes mitochondrial substrate oxidation resulting in slower ATP production than from glycolytic reliance thereby reducing cellular ATP content (see Fig. 5). Cellular ATP content is reduced further by concurrent increases in mitochondrial uncoupling protein activity, resulting in heat dissipation and lower mitochondrial ATP synthase activity; observations supported by leucine induction of uncoupling protein 3 in C2C12 myocytes (Sun and Zemel 2009). Elevated UCP activity causes similar effects to potent chemical uncoupling agents causing reduced ATP content, a potent metabolic stimulus leading to increased mitochondrial content (Rohas et al. 2007; Vaughan et al. 2012b). Interestingly, our observations demonstrate how leucine treatment can differentially influence cellular ATP content between the two cell models. Specifically, leucine diminished ATP content of non-malignant C2C12 mouse myoblasts, but did not significantly alter ATP content of human sarcoma cells; a discrepancy which may be a result of the cancerous phenotype of the RD cells with their increased reliance on glycolytic metabolism (see Fig. 3) (Hanahan and Weinberg 2011).
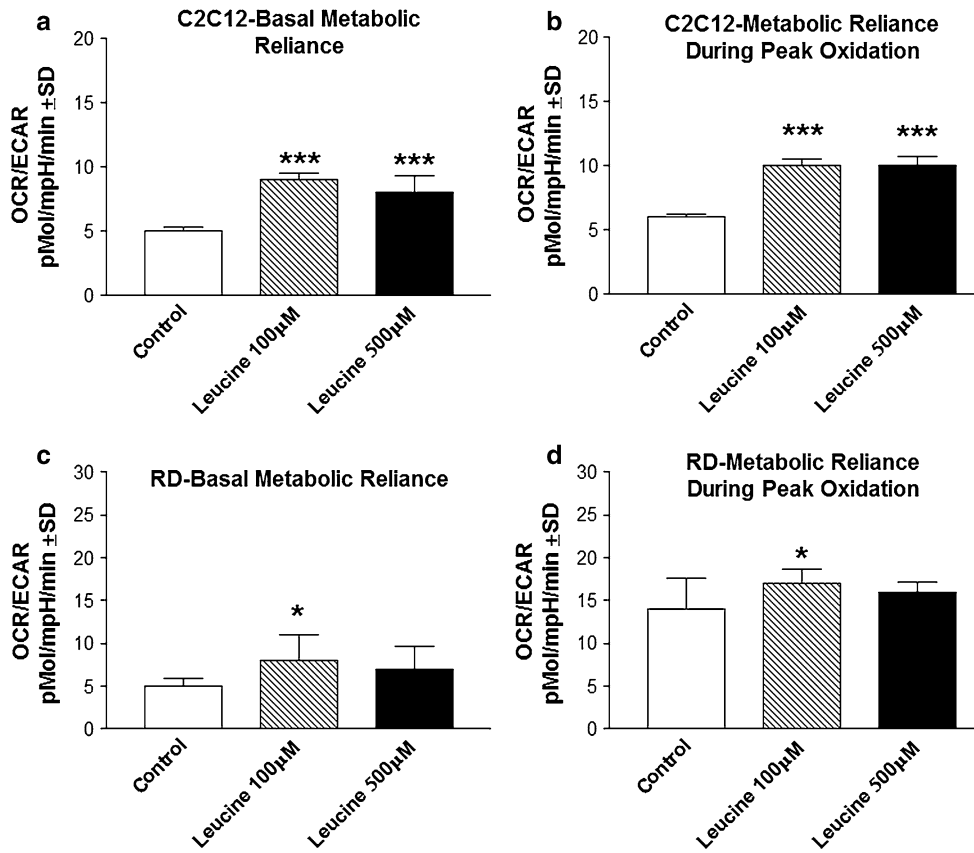
Fig. 4 Oxidative reliance. **a** Basal oxidative reliance expressed as a ratio of oxygen consumption rate (OCR) to extracellular acidification rate (ECAR) of C2C12 cells treated with either 100 or 500 μM for 24 h. 95 % CI = control vs. leucine 100 μM: −4.751 to −3.249 and control vs. leucine 500 μM: −3.751 to −2.249. **b** Peak oxidative reliance of C2C12 cells treated as described above for 24 h. 95 % CI = control vs. leucine 100 μM: −4.677 to −3.323 and control vs. leucine 500 μM: −4.677 to −3.323. **c** Basal oxidative reliance of RD cells treated with either 100 or 500 μM for 24 h. 95 % CI = control vs. leucine 100 μM: −5.110 to −0.8898 and control vs. leucine 500 μM: −4.110 to 0.1102. **d** Peak oxidative reliance of RD cells treated as described above. 95 % CI = control vs. leucine 100 μM: −5.102 to −0.8977 and control vs. leucine 500 μM: −4.102 to 0.1023. *$p < 0.05$, **$p < 0.01$, and ***$p < 0.001$ significantly greater than control
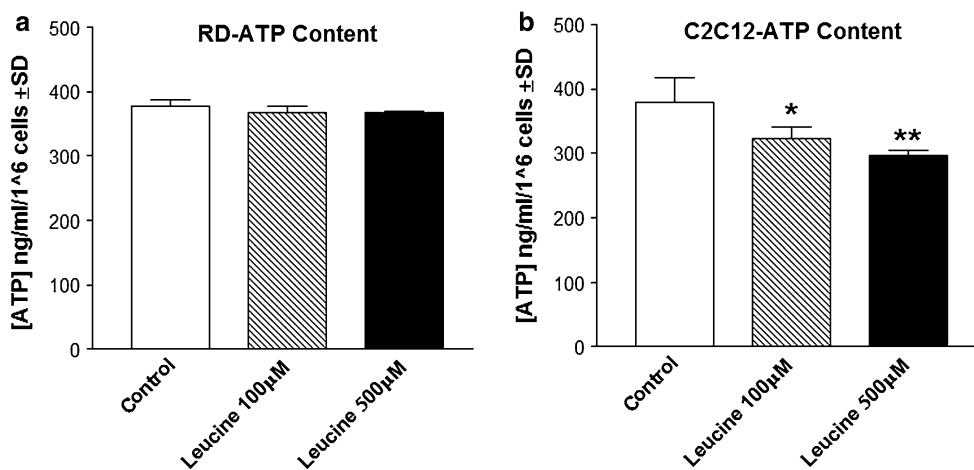

Fig. 5 Cellular ATP concentration. **a** Cellular ATP content expressed as ATP concentration/million cells of rhabdomyosarcoma cells (RD) treated with either 100 or 500 μM of leucine or control for 48 h. 95 % CI = control vs. leucine 100 μM: −4.326 to 27.49 and control vs. leucine 500 μM: −5.730 to 26.09. **b** Cellular ATP content of mouse myoblast cells (C2C12) treated with either 100 or 500 μM of leucine or control for 48 h. 95 % CI = control vs. leucine 100 μM: 5.752 to 105.6 and control vs. leucine 500 μM: 31.03 to 130.9. *$p < 0.05$, **$p < 0.01$, and ***$p < 0.001$ compared with control
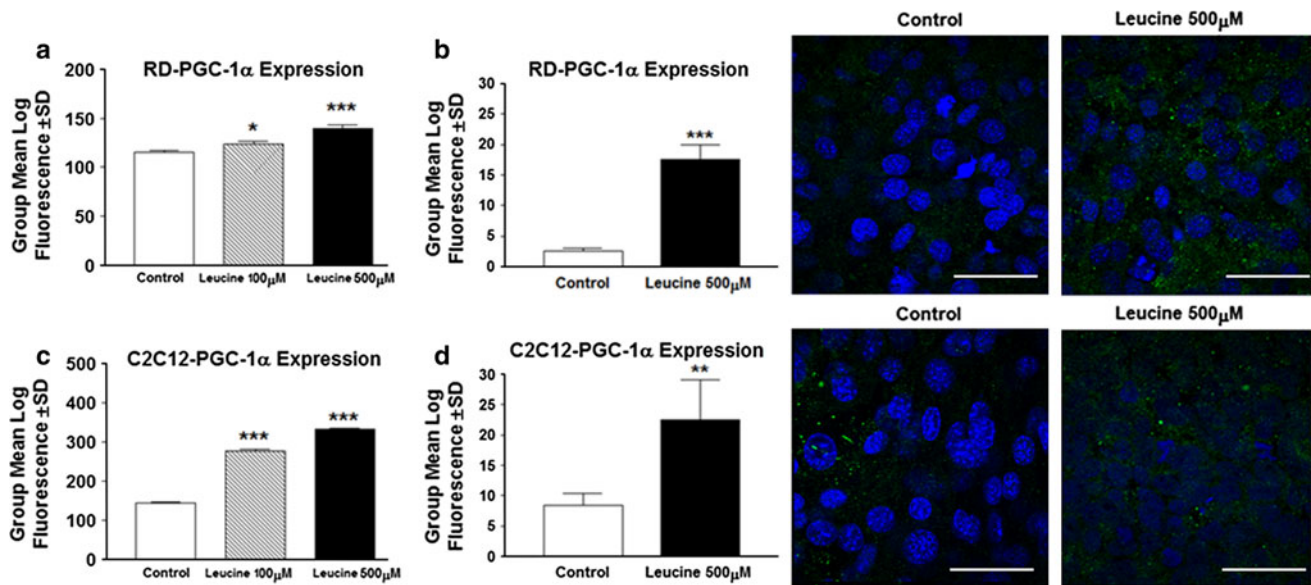
Fig. 6 PGC-1α protein. **a** Group mean log fluorescence from flow cytometry of rhabdomyosarcoma cells (RD) treated as described in "Methods" and stained with PGC-1α primary antibody and Alexa-Fluor 488 secondary antibody. 95 % CI = control vs. leucine 100 μM: -15.71 to -0.9584 and control vs. leucine 500 μM: -31.71 to -16.96. **b** Group mean log fluorescence of confocal microscopy of RD cells treated as described in "Methods" and stained with PGC-1α primary antibody and AlexaFluor 488 secondary antibody (green) and DAPI (blue) (quantification was performed with $N = 7$ per treatment). **c** Group mean log fluorescence from flow cytometry of C2C12 cells treated as described in "Methods" and stained with PGC-1α primary antibody and AlexaFluor 488 secondary antibody. 95 % CI = control vs. leucine 100 μM: -139.1 to -128.2 and control vs. leucine 500 μM: -193.5 to -182.5. **d** Group mean log fluorescence of confocal microscopy of C2C12 cells treated as described in "Methods" and stained with PGC-1α primary antibody and AlexaFluor 488 secondary antibody (green), DAPI (blue) and white line corresponds to 50 μm. Quantification was performed with $N = 7$ per treatment. $*p < 0.05$, $**p < 0.01$, and $***p < 0.001$ compared with control (color figure online)

Other observations demonstrate that leucine stimulates SIRTI, which is also capable of inducing mitochondrial biosynthesis (Sun and Zemel 2009). Cultured myocytes and adipocytes demonstrate convincing increases in mitochondrial biosynthesis with accompanying increases in SIRT1 activity and expression using an ex vivo–in vitro approach, although the authors acknowledge that leucine or leucine metabolites could be responsible for observed effects (Bruckbauer and Zemel 2011). It is also conceivable that increased protein synthesis raises cellular ATP needs contributing to reductions in cellular energy availability leading to increased mitochondrial content (although protein synthesis was not measured in our study). Figure 10 summarizes the proposed interactions and effects of leucine treatment on skeletal muscle cells.

Although there is inconclusive evidence that the addition of leucine to a diet with adequate/excess energy and protein provides any additional benefit, leucine may provide some added benefit for energy-restricted (weight loss) diets. Specifically, additional leucine to caloric restriction may improve muscle oxidative capacities as

our work demonstrates, while simultaneously preserving lean tissue and promotion of protein synthesis (observations which must be verified experimentally). Our observations, although preliminary, support the hypothesis that leucine might be an effective agent for heightening oxidative metabolism and oxidative capacity in skeletal muscle.

Conclusion

Leucine is a potent and essential dietary component, which has been heavily researched for its role in muscle protein synthesis via an mTOR mediated pathway. Our work uniquely demonstrates that leucine increases energy expenditure in skeletal muscle cells, although the precise nature of these heightened energy costs remains ill-defined. Our observations support the hypothesis that leucine may function to increase energy expenditure, although further exploration into the mechanism of action and link between leucine-induced energy expenditure and protein synthesis is necessary.
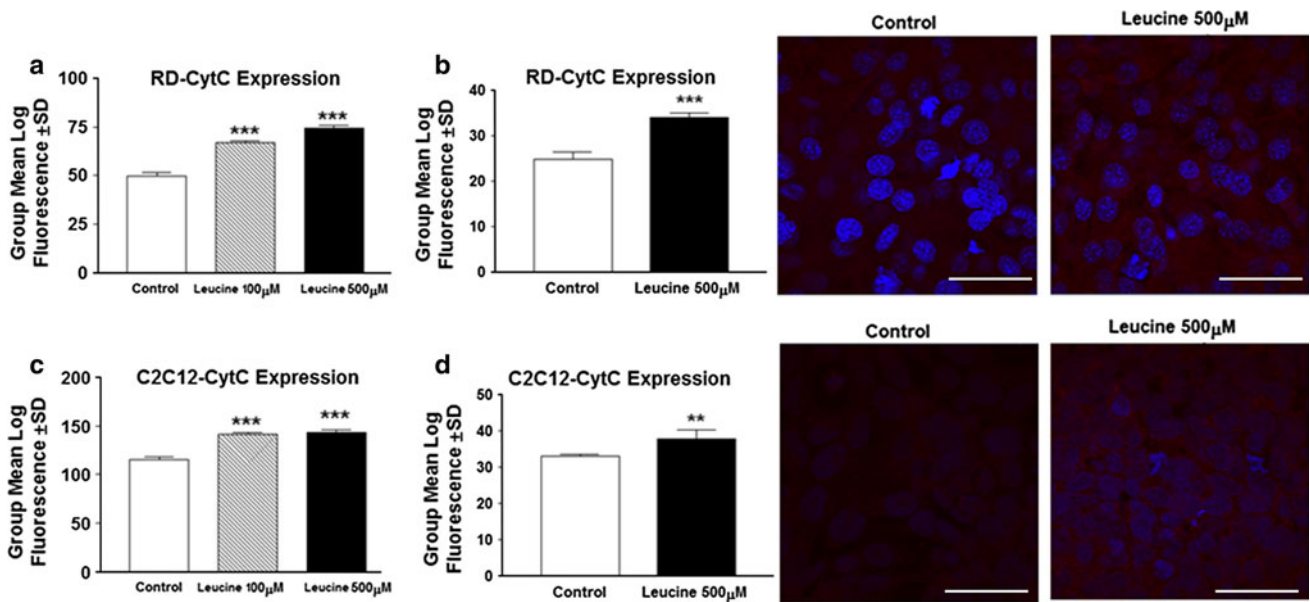
Fig. 7 Cytochrome C protein. **a** Group mean log fluorescence from flow cytometry of rhabdomyosarcoma cells (RD) treated as described in "Methods" and stained with cytochrome C primary antibody and AlexaFluor 488 secondary antibody. 95 % CI = control vs. leucine 100 µM: −21.34 to −13.33 and control vs. leucine 500 µM: −28.67 to −20.66. **b** Group mean log fluorescence of confocal microscopy of RD cells treated as described in "Methods" and stained with cytochrome C primary antibody and AlexaFluor 633 secondary antibody (red) and DAPI (blue) (quantification was performed with N = 7 per treatment). **c** Group mean log fluorescence from flow cytometry of C2C12 cells treated as described in "Methods" and stained with cytochrome C primary antibody and AlexaFluor 488 secondary antibody. 95 % CI = control vs. leucine 100 µM: −32.58 to −19.42 and control vs. leucine 500 µM: −34.24 to −21.09. **d** Group mean log fluorescence of confocal microscopy of C2C12 cells treated as described in "Methods" and stained with cytochrome C primary antibody and AlexaFluor 633 secondary antibody (red), DAPI (blue), and white line corresponds to 50 µm. Quantification was performed with N = 7 per treatment. *p < 0.05, **p < 0.01, and ***p < 0.001 compared with control (color figure online)
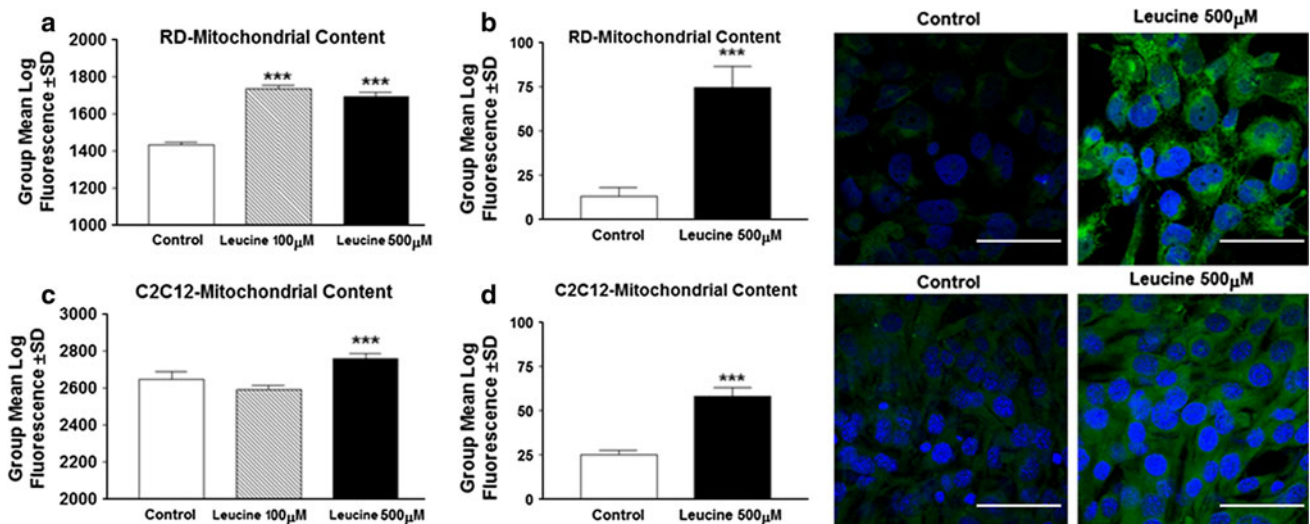

Fig. 8 Mitochondrial content. **a** Group mean log fluorescence from flow cytometry of rhabdomyosarcoma cells (RD) treated as described in "Methods" and stained Mitotracker Green. 95 % CI = control vs. leucine 100 µM: −335.3 to −271.1 and control vs. leucine 500 µM: −294.3 to −230.1. **b** Group mean log fluorescence of confocal microscopy of RD cells treated as described in "Methods" and stained with Mitotracker (green) and DAPI (blue) (quantification was performed with N = 7 per treatment). **c** Group mean log fluorescence from flow cytometry of C2C12 cells treated as described in "Methods" and stained with Mitotracker. 95 % CI = control vs. leucine 100 µM: 3.368–113.4 and control vs. leucine 500 µM: −164.0 to −53.97. **d** Group mean log fluorescence of confocal microscopy of C2C12 cells treated as described in "Methods" and stained with Mitotracker (green) DAPI (blue), and white line corresponds to 50 µm. Quantification was performed with N = 7 per treatment. *p < 0.05, **p < 0.01, and ***p < 0.001 compared with control (color figure online)

Fig. 9 Cell viability. **a** WST-1 cell viability following treatment of C2C12 cells with either leucine at 100 or 500 μM for 48 h. **b** Cell viability of RD cells following treatment as described above for 48 h
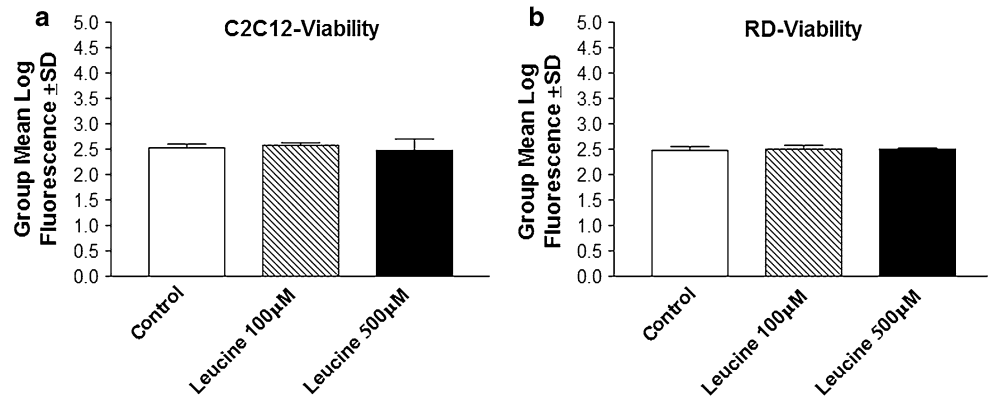

Fig. 10 Proposed role of leucine in the stimulation of PGC-1α expression leading to mitochondrial biosynthesis. *AMPK* 5' AMP-activated protein kinase, *CAC* citric acid cycle, *FOXO1* forkhead box protein, *mTOR* mammalian target of rapamycin, *PGC-1α* peroxisome proliferator-activated receptor coactivator 1 alpha, *SIRT1* silent information regulator transcript 1, and *UCP* uncoupling protein
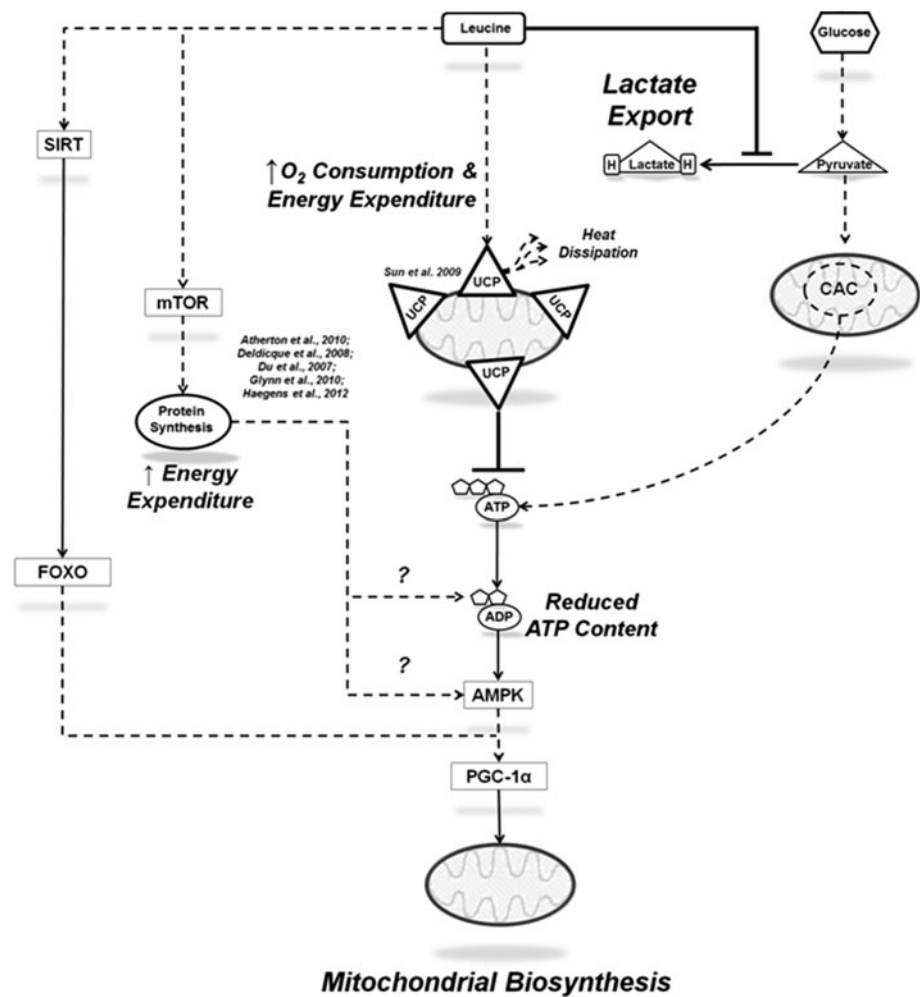
References

Araki M, Maeda M, Motojima K (2012) Hydrophobic statins induce autophagy and cell death in human rhabdomyosarcoma cells by depleting geranylgeranyl diphosphate. Eur J Pharmacol 674:95–103

Armoni M, Quon MJ, Maor G, Avigad S, Shapiro DN, Harel C, Esposito D, Goshen Y, Yaniv I, Karnieli E (2002) PAX3/Forkhead homolog in rhabdomyosarcoma oncoprotein activates glucose transporter 4 gene expression in vivo and in vitro. J Clin Endocrinol Metab 87:5312–5324

Atherton PJ, Smith K, Etheridge T, Rankin D, Rennie MJ (2010) Distinct anabolic signalling responses to amino acids in C2C12 skeletal muscle cells. Amino Acids 38:1533–1539

Bruckbauer A, Zemel MB (2011) Effects of dairy consumption on SIRT1 and mitochondrial biogenesis in adipocytes and muscle cells. Nutr Metab 8:91

Deldicque L, Canedo CS, Horman S, De Potter I, Bertrand L, Hue L, Francaux M (2008) Antagonistic effects of leucine and glutamine on the mTOR pathway in myogenic C2C12 cells. Amino Acids 35:147–155

Du M, Shen QW, Zhu MJ, Ford SP (2007) Leucine stimulates mammalian target of rapamycin signaling in C2C12 myoblasts in part through inhibition of adenosine monophosphate-activated protein kinase. J Anim Sci 85:919–927

Giulivi C, Ross-Inta C, Horton AA, Luckhart S (2008) Metabolic pathways in Anopheles stephensi mitochondria. Biochem J 415:309–316

Glynn EL, Fry CS, Drummond MJ, Timmerman KL, Dhanani S, Volpi E, Rasmussen BB (2010) Excess leucine intake enhances muscle anabolic signaling but not net protein anabolism in young men and women. J Nutr 140:1970–1976

Haegens A, Schols AM, van Essen AL, van Loon LJ, Langen RC (2012) Leucine induces myofibrillar protein accretion in cultured skeletal muscle through mTOR dependent and -independent control of myosin heavy chain mRNA levels. Mol Nutr Food Res 56:741–752

Hanahan D, Weinberg RA (2011) Hallmarks of cancer: the next generation. Cell 144:646–674

Lendoye E, Sibille B, Rousseau AS, Murdaca J, Grimaldi PA, Lopez P (2011) PPAR beta activation induces rapid changes of both AMPK subunit expression and AMPK activation in mouse skeletal muscle. Mol Endocrinol 25:1487–1498

Pagel-Langenickel I, Bao JJ, Joseph JJ, Schwartz DR, Mantell BS, Xu XL, Raghavachari N, Sack MN (2008) PGC-1 alpha integrates insulin signaling, mitochondrial regulation, and bioenergetic function in skeletal muscle. J Biol Chem 283:22464–22472

Philp A, Belew MY, Evans A, Pham D, Sivia I, Chen A, Schenk S, Baar K (2011) The PGC-1 alpha-related coactivator promotes mitochondrial and myogenic adaptations in C2C12 myotubes. Am J Physiol Regul Integr Comp Physiol 301:R864–R872

Rohas LM, St-Pierre J, Uldry M, Jager S, Handschin C, Spiegelman BM (2007) A fundamental system of cellular energy homeostasis regulated by PGC-1 alpha. Proc Natl Acad Sci USA 104:7933–7938

Singh P, Kohr D, Kaps M, Blaes F (2010) Skeletal muscle cell MHC I expression: implications for statin-induced myopathy. Muscle Nerve 41:179–184

Sun X, Zemel MB (2007) Leucine and calcium regulate fat metabolism and energy partitioning in murine adipocytes and muscle cells. Lipids 42:297–305

Sun X, Zemel MB (2009) Leucine modulation of mitochondrial mass and oxygen consumption in skeletal muscle cells and adipocytes. Nutr Metab 6:26

Vaughan RA, Garcia-Smith R, Bisoffi M, Conn CA, Trujillo KA (2012a) Conjugated linoleic acid or omega 3 fatty acids increase mitochondrial biosynthesis and metabolism in skeletal muscle cells. Lipids Health Dis 11:142

Vaughan RA, Garcia-Smith R, Bisoffi M, Trujillo KA, Conn CA (2012b) Effects of caffeine on metabolism and mitochondria biogenesis in rhabdomyosarcoma cells compared with 2,4-dinitrophenol. Nutr Metab Insights 5:59

Vaughan RA, Garcia-Smith R, Bisoffi M, Trujillo KA, Conn CA (2012c) Treatment of human muscle cells with popular dietary supplements increase mitochondrial function and metabolic rate. Nutr Metab 9:101

Wikstrom JD, Sereda SB, Stiles L, Elorza A, Allister EM, Neilson A, Ferrick DA, Wheeler MB, Shirihai OS (2012) A novel high-throughput assay for islet respiration reveals uncoupling of rodent and human islets. PLoS One 7:e33023

Zhang Y, Guo K, LeBlanc RE, Loh D, Schwartz GJ, Yu YH (2007) Increasing dietary leucine intake reduces diet-induced obesity and improves glucose and cholesterol metabolism in mice via multimechanisms. Diabetes 56:2174–2177